New Host Factors Important for Respiratory Syncytial Virus (RSV) Replication Revealed by a Novel Microfluidics Screen for Interactors of Matrix (M) Protein

Sarit Kipper, Samar Hamad, Leon Caly, Dorit Avrahami, Eran Bacharach, David A. Jans, Doron Gerber, Monika Bajorek

New Host Factors Important for Respiratory Syncytial Virus (RSV) Replication Revealed by a Novel Microfluidics Screen for Interactors of Matrix (M) Protein*[S]

Sarit Kipper‡, Samar Hamad§, Leon Caly¶, Dorit Avrahami‡, Eran Bacharach‖, David A. Jans¶, Doron Gerber‡‡**, and Monika Bajorek§‡‡**

Although human respiratory syncytial virus (RSV) is the most common cause of bronchiolitis and pneumonia in infants and elderly worldwide, there is no licensed RSV vaccine or effective drug treatment available. The RSV Matrix protein plays key roles in virus life cycle, being found in the nucleus early in infection in a transcriptional inhibitory role, and later localizing in viral inclusion bodies before coordinating viral assembly and budding at the plasma membrane. In this study, we used a novel, high throughput microfluidics platform and custom human open reading frame library to identify novel host cell binding partners of RSV matrix. Novel interactors identified included proteins involved in host transcription regulation, the innate immunity response, cytoskeletal regulation, membrane remodeling, and cellular trafficking. A number of these interactions were confirmed by immunoprecipitation and cellular colocalization approaches. Importantly, the physiological significance of matrix interaction with the actin-binding protein cofilin 1, caveolae protein Caveolin 2, and the zinc finger protein ZNF502 was confirmed. siRNA knockdown of the host protein levels resulted in reduced RSV virus production in infected cells. These results have important implications for future antiviral strategies aimed at targets of RSV matrix in the host cell. ***Molecular & Cellular Proteomics 14: 10.1074/mcp. M114.044107, 532–543, 2015.***

From the ‡Nanotechnology Institute, Mina and Evrard Goodman Faculty of Life Sciences, Bar Ilan University, Ramat Gan, Israel; §Section of Virology, Faculty of Medicine, Imperial College London, London, UK; ¶Department of Biochemistry and Molecular Biology, Monash University, Melbourne, Australia; ‖Department of Cell Research and Immunology, Tel Aviv University, Israel

Received, August 26, 2014 and in revised form, December 29, 2014
Published, MCP Papers in Press, January 2, 2015, DOI 10.1074/mcp.M114.044107

Author contributions: S.K., D.A., E.B., D.A.J., D.G., and M.B. designed research; S.K., S.H., L.C., and M.B. performed research; D.A. contributed new reagents or analytic tools; S.K., S.H., L.C., D.A., D.A.J., D.G., and M.B. analyzed data; D.A.J., D.G., and M.B. wrote the paper.

Although human respiratory syncytial virus (RSV)[1], from the *Pneumovirus* genus of the *Paramyxoviridae* family, is the most common cause of infantile bronchiolitis and pneumonia in the developed world, there is no vaccine or antiviral therapy available to combat it (1–4). The RSV Matrix (M) protein plays key roles in virus life cycle. Early in infection M localizes in the nucleus via the action of the nuclear transport protein Importin β1 (5), serving an apparent dual role of inhibiting host cell transcription (6) as well as preventing inhibition of viral transcription in the cytoplasm (7). Nuclear targets of M have thus far not been reported. Later in infection, M traffics to the cytoplasm through the action of the nuclear export protein CRM-1 (8) to associate with inclusion bodies (IBs), the site of RSV transcription and replication. It was recently suggested that M also serves to sequester cellular proteins involved in the host innate immune response (9). M localization into IBs is dependent on the RSV protein M2–1 and is believed to represent a potential switch between viral transcription and assembly (10), with M helping coordinate the latter in an adaptor role. M association in IBs with the RSV F (fusion) protein triggers immediate filament formation (11). Ultimately, all of the viral proteins localize at the apical cell surface, where M helps coordinate assembly into virus filaments followed by budding (12, 13).

The minimal RSV viral protein requirement for filament formation and budding of virus-like particles (VLPs) are F, M, nucleo (N), and phospho (P) protein (14). Little is known regarding the specific roles of P and N in budding, but the cytoplasmic tail of F appears to be critical to filament formation, presumably through recruiting specific host factor(s) required for virus release (14, 15). M's crucial role in viral filament maturation and elongation relates to the transfer of RNP

[1] The abbreviations used are: RSV, Respiratory Syncytial Virus; M, Matrix protein; F, Fusion protein; N, Nucleo protein; P, Phospho protein; IB, Inclusion Bodies; RNP, Ribo Nucleo Protein; ARE, Apical Recycling Endosomes; NDV, Newcastle Disease Virus; MOI, Multiplicity of Infection; PING, Protein Interaction Network Generator; ORF, Open Reading Frame; FBS, Fetal Bovine Serum; BSA, Bovine Serum Albumin; PFA, Paraformaldehyde; LSM, Laser Scanning Microscope; ZNF, Zinc Finger proteins.

complexes from IBs to the sites of budding (16). We recently showed that ordered oligomerization of M is central to infectious filamentous virus production (17), potentially through providing the framework for filament morphology (18), in conjunction with M2–1, which serves as a bridging protein between the oligomeric M layer and RNP in the mature virus (19).

Additional to the crucial role of M in RSV filament morphology and infectivity, M has been suggested to recruit cellular factor(s) during virus assembly (20–23). Proteins involved in apical recycling endosomes (ARE)-mediated protein sorting (*e.g.* Myosin 5 beta), have been shown to be essential for RSV assembly (24) with budding of released virus believed to be Vps4-independent and to require Rab11a FIP2 protein (25). However, only Importin-β1 (5) and CRM1 (8) (see above) are known to be direct interactors of M. A proteomic screen for cellular interactors of RSV M, N, and F proteins identified only limited numbers of proteins, none of which could be validated to bind directly to M (26). Overall, the network of RSV-cell interactions is still mostly unknown, with limited targets identified.

Protein microarrays technology allows the interrogation of protein–protein interactions, which could possibly overcome the obstacles mentioned above (27). Here we use an *in vitro* protein expression and interaction analysis platform based on a highly parallel and sensitive microfluidics affinity assay (28) to identify new host factors interacting with RSV M. This is the first time microfluidics has been used to screen for host factors interacting with a protein from a negative strand RNA virus. A range of factors were identified for the first time, including proteins involved in host transcription and translation regulation, innate immunity response, plasma membrane remodeling, cytoskeleton regulation, and cellular trafficking, with a number verified by coprecipitation. Of these, we present initial characterization of key caveolae structural component Caveolin (Cav) and the actin-binding protein Cofilin1 (Cof1) as cellular factors that colocalize with M in viral inclusions and filaments, and of the zinc finger protein ZNF502, which appears to interact with RSV M in the nucleus. These and the other host factor-RSV M interactions identified here for the first time may be exciting possibilities as targets for anti-RSV approaches in the future.

EXPERIMENTAL PROCEDURES

Microfluidics—The microfluidic devices were fabricated on silicone molds performed as described previously (29, 30). To prevent nonspecific adsorption and to control suitable binding orientation, all of the accessible surface area within the microfluidic device was chemically modified. Biotinylated-BSA (1 μg/μl, Pierce, Tel Aviv, Israel) was flowed for 20 min through the device, allowing binding of the BSA to the epoxy surface. Strepavidin (0.5 μg/μl) (Neutravidin, Pierce) was then added for 20 min. The "button" valve was then closed and biotinylated-BSA was flowed over once again as above. Following the passivation step, the "button" valve was released and the appropriate anti-penta-His (Qiagen, Valencia, CA) or -V5 (Pierce) biotinylated antibody applied at concentrations of 0.1–0.2 mg/ml enabling binding to exposed Strepavidin, specifically activating the area under the "button" (30). Hepes (50 mM, Biological Industries, Kibbutz Beit Haemek, Israel) was used for washing unreacted substrates between each of the surface chemistry steps.

Protein Network Interaction Generator (PING)—Proteins were expressed on the device or in a test tube (small evaluation screens) using an expression mix of rabbit reticulocyte quick coupled transcription and translation reaction (Promega, Madison, WI). In this study, coding regions for 500 proteins from the human proteome were assembled using PCR (30) and selected clones from the public genome-scale lentiviral sequence-confirmed expression library of human ORFs (open reading frames) in a Gateway vector system (31) as templates. PCR products were generated by using specific primers encoding c-Myc and Penta-His tags at the N and C-terminal, respectively, for all of the ORFs. The linear synthetic genes were spotted onto the glass substrate and the microfluidic device attached to the array. Protein expression on the device was performed by flushing the device with 12.5 μl of the expression mix, following opening of the "neck valve," to initiate *in vitro* transcription/translation of all of the proteins in parallel. The "sandwich" valves were then closed to isolate each unit cell from its environment, and the device incubated on a hot plate for 2.5 h at 32 °C. Expressed proteins then diffused through the DNA chamber to the reaction chamber and immobilized to the surface via binding of the C-terminal Penta-His tag to the appropriate surface-attached antibody under the "button" area. Proteins were labeled fluorescently using 0.01 mg/ml Cy3-labeled anti-c-Myc antibody (Sigma, St. Louis, MO).

In small evaluation screens, PCR-generated human ORF linear expression templates were added directly to rabbit reticulocyte lysate off-chip in the presence of a FluoroTect™ GreenLys (Promega) *in vitro* Translation Labeling System for labeling and detection of proteins synthesized in a final volume of 25 μl rabbit reticulocyte lysate and 1 μg of the relevant DNA in an Eppendorf microfuge tube. After incubation at 32 °C for 2.5 h with agitation (600 rpm), proteins were flushed into the device to allow binding to the surface.

RSV M protein was produced after cloning of the coding sequence into the pCAG vector using the same PCR approach as above, but with C-terminal primer encoding the V5 tag. For all experiments, RSV M was generated by *in vitro* transcription/translation from the linear PCR fragment in a final volume of 25 μl in an Eppendorf microfuge tube, which was then incubated as above, before flushing into the device as above.

Analysis of Microfluidics—Interaction ratios are defined as the fluorescence ratio for RSV M and the surface bound human protein based on the extent of labeling by 0.01 mg/ml of Alexa 647-labeled anti-V5 (Abd-Serotec, Oxford, UK) and Cy3-labeled anti-c-Myc (Sigma) antibodies, respectively. Measurements were performed using a microarray scanner (LS Reloaded, Tecan) with fluorescent excitation at 635 nm (for RSV M) and 575 nm (for human proteins). In small screens, human proteins were expressed in presence of fluorescent Lys (FluoroTect™ GreenLys, Promega) and protein expression levels determined with a microarray scanner (LS Reloaded, Tecan) with fluorescent excitation at 488 nm, where the signals were normalized to the number of lysines in each protein (30).

Cell Culture and RSV Virus Preparation—HEp-2 (ATCC CCL-23™), 293T, and Vero cells (both cell lines were provided by W. Barclay, Imperial College London) were maintained in DMEM medium (Invitrogen, Grand Island, NY) supplemented with 10% fetal bovine serum (FBS, Invitrogen), 1% l-glutamine, and 1% penicillin-streptomycin. The transformed human bronchial epithelial cell line BEAS-2B (ATCC) was maintained in RPMI 1640 medium (Invitrogen) supplemented with 10% fetal bovine serum (FBS, Invitrogen), 1% L-glutamine, and 1% penicillin-streptomycin. Transfections were performed with Lipofectamine 2000 (Invitrogen) used according to the manufacturer's specifications. Plaque-purified human RSV (A2 strain from ATCC) or

recombinant (r) A2 RSV strain was cultured in Vero cells. In the case of cell-associated virus, the culture supernatant was removed when extensive cytopathic effects were observed, and the cells resuspended in serum free SPGA media (218 mM sucrose, 7.1 mM K_2HPO_4, 4.9 mM sodium glutamate, and 1% BSA), followed by centrifugation (1300 × *g*, 15 min, 4 °C) and storage at −80 °C. RSV titers were determined by immune-plaque assay in triplicate on HEp-2 cells.

Calcium Phosphate Transfection—Overnight cultures of 293T cells, seeded at 1×10^6 cells/60 mm plate in 5 ml DMEM/10% FBS, were transfected with 4 μg of each plasmid. Plasmid DNA was added to sterile H_2O to 215 μl total volume. In a separate Eppendorf microfuge tube 250 μl of 2×HeBS buffer (42 mM Hepes, 270 mM NaCl, 1 mM KCl, and 10 mM Dextrose, pH 7.1) was mixed with 5 μl 100×PO_4 (1.4 mM Na_2HPO_4). Diluted DNA was mixed with the HeBS/PO_4 solution, 30 μl of 3.2 M $CaCl_2$ was added gently, and the mix was immediately added to cells. Media was changed after 6 h and cells were harvest 36 h post-transfection for immune-precipitation assay.

Immune-plaque Assay—Overnight cultures of HEp-2 (seeded at 4×10^4 cell/well in 96-well plate) were infected with virus stocks diluted in a separate 96-well plate using doubling dilutions in serum-free DMEM media, starting at 1/10 for supernatant virus and 1/50 for cell-associated virus. Cells were washed once with serum-free DMEM, and 50 μl of each of the virus dilution added to triplicate wells and left for 2 h at 37 °C. One hundred microliters of 2% FBS DMEM was then added and the plates incubated for further 48 h at 37 °C. In the case of immunostaining, medium was discarded and the cells washed in 100 μl phosphate buffered saline (PBS) and fixed for 20 min with 100 μl absolute methanol containing 2% hydrogen peroxide. After washing with 200 μl PBS/1% BSA, cells were incubated with biotinylated anti-RSV antibody (1:500, AbD Serotec) for 2 h, washed three times in PBS/1% BSA, and then stained with ExtrAvidin peroxidase (1:500, Sigma) for 2 h in the dark. Cells were washed three times and plaques visualized using Sigma Fast Diaminobenzidine (DAB) Peroxidase Substrate (Sigma).

Viral Plaque Assay (PFA Fixation/Crystal Violet)—Overnight cultures of Vero cells were seeded at a density of 2×10^5 cells/well in 24-well plates to form an even monolayer. Viral stocks to be assayed were serially diluted 1:10 (50 μl into 450 μl DMEM 2% FCS) from 10^{-1} to 10^{-5} and 200 μl used to infect duplicate wells. Infected cells were placed at 37 °C for 2 h then washed with DMEM/2% FCS then overlaid with 500 μl of 0.8% AquacideII/DMEM 2% FCS and incubated at 37 °C for 4–6 days. Cells were fixed with 4% Paraformaldehyde (PFA) for 12 h then stained with 0.4% Crystal Violet/20% Methanol in PBS. Plaques were then imaged on an Olympus SX61 Microscope.

Visualization of Virus-like Filaments—Overnight cultures of HEp-2 cells (seeded at 4×10^5 cells/well in 6-well plates on 16-mm glass coverslips) were transfected to express plasmids (0.4 μg each) encoding the RSV A2 WT M protein along with pcDNA3.1 codon optimized plasmids encoding the RSV A2 N, P, and F, using Lipofectamine 2000 (Invitrogen). Cells were fixed 24 h post-transfection, immunostained, and imaged as described below.

RSV Infection for Infectivity Assay and Viral Filament Visualization—Overnight cultures of HEp-2 or BEAS-2B cells, seeded at 4×10^5 cells/well in 6-well plates with or without 16 mm glass coverslips, were infected with recombinant RSV WT (rA2) or WT RSV at a multiplicity of infection (MOI) of three. Cells were fixed 24 h postinfection, immunostained and imaged as described below, to visualize filaments. For infectivity assay, cell-associated and released virus fractions were harvested and virus titers of cell-associated and supernatant fractions were determined using the immune-plaque assay or PFA fixation/Crystal Violet assay (above).

Immunostaining and Imaging—Cells were fixed with 4% paraformaldehyde in PBS for 10 min, blocked with 3% BSA in 0.2% Triton X/PBS for 10 min, and coimmunostained with monoclonal anti-M (1:200, gift from Mariethe Ehnlund, Karolinska Institute, Sweden), polyclonal anti-RSV (1:200, Abcam, Cambridge, UK), monoclonal anti-Myc (1:500, Abcam), polyclonal anti-Myc (1:100, Abcam), polyclonal anti-Cav1 (1:500, Abcam), polyclonal anti-Cav2 (1:50, Abcam), or polyclonal anti-Cof1 (1:500, Abcam) antibodies followed by species specific secondary antibodies conjugated to Alexa Fluor 488 and Alexa Fluor 568 (1:1000, Invitrogen). Images were obtained on Zeiss 5 PASCAL confocal laser scanning microscope (LSM) using 63×/1.4 Plan-Apochromat oil lens (averaging 4×). Images were acquired using Zeiss LSM Image Browser software (4.2.0.121, Zeiss, Cambridge, UK).

Coprecipitation Experiments with One-STREP-FLAG (OSF) Tagged M—293T cells were seeded (1.5×10^6 cells/60 mm dish) and cotransfected with 4 μg of each of the relevant expression plasmids using the calcium phosphate method (above). Cells were harvested 36 h post-transfection and lysed in 300 μl lysis buffer (50 mM Tris, pH 7.4, and 150 mM NaCl) supplemented with protease inhibitor mixture (Sigma) and 1% Triton X-100 for 10 min. Lysates were clarified by centrifugation (11,600 × *g*, 6 min, 4 °C), and streptactin-tagged proteins affinity purified by incubation with StrepTactin Sepharose for 2h (40 μl slurry, Qiagen). The beads were washed three times in wash buffer (20 mM Tris, pH 7.4, and 150 mM NaCl) supplemented with 0.1% Triton X-100, and bound proteins detected by Western blot.

Small Interfering RNA (siRNA) Depletion—For knockdown of Caveolin1, Caveolin2, and Cofilin1, overnight cultures of HEp-2 cells were seeded at 4×10^5 cells/well in six-well plates or 2×10^5 cells/well in 12-well plates on 16 mm glass coverslips and siRNA depletion experiments were performed 24 h later with siRNA (20 nM Qiagen FlexiTube siRNA using Lipofectamine RNAiMax, Invitrogen), the medium changed 6 h later, and the cells infected at 48 h after siRNA treatment with WT A2 RSV at an MOI of three. Cells and supernatant were harvested 24 h later for Western blot and virus titer (cell associated and released virus) analysis and/or immunostaining.

In the case of ZNF502 knockdown, sub-confluent monolayers of 293T were seeded into 12-well plates overnight. Cells were transfected with 20 nM ZNF502 SMARTPool siRNA or negative control siRNA (Dharmacon, Mulgrave, Australia) using 2 μl DharmaFECT1 transfection reagent as recommended by the manufacturer. Forty-eight hours post transfection, cells were infected with (r) A2 RSV strain at an MOI of one, and cell associated and supernatant released virus was harvested for analysis by plaque assay 24 h postinfection.

SDS-PAGE and Western Blotting—Protein samples were analyzed on 12% polyacrylamide gels and subjected to electrophoresis in Tris-glycine buffer. All samples were boiled for 3 min prior to electrophoresis. Gels were then transferred to PVDF membrane (Roche Diagnostics, Sussex, UK). The blots were blocked with 5% nonfat milk in Tris-buffered saline (pH 7.4) followed by incubation in monoclonal anti-Myc (9E10 hybridoma), monoclonal anti-FLAG (1:1000, Sigma), polyclonal anti-Cofilin1 (1:1000, Abcam), polyclonal anti-Caveolin1 (1:1000, Abcam), polyclonal anti-Caveolin2 (1:1000, Abcam), polyclonal anti-ZNF502 (1:1000, Abcam), or monoclonal anti-β actin (1:500, Abcam), and horseradish peroxidase (HRP)-conjugated goat anti-mouse or goat anti-rabbit antibody (1:10000, Invitrogen). Western blots were developed using freshly prepared chemiluminescent substrate (100 mM Tris-HCl, pH 8.8, 1.25 mM luminol, 0.2 mM p-coumaric acid, and 0.05% H_2O_2) and exposed to FUJI autoradiography films.

RESULTS

High Throughput Screen for M-host Interactions using Microfuidics—We performed a high-throughput microfluidics-based screen (see Experimental Procedures section for de-

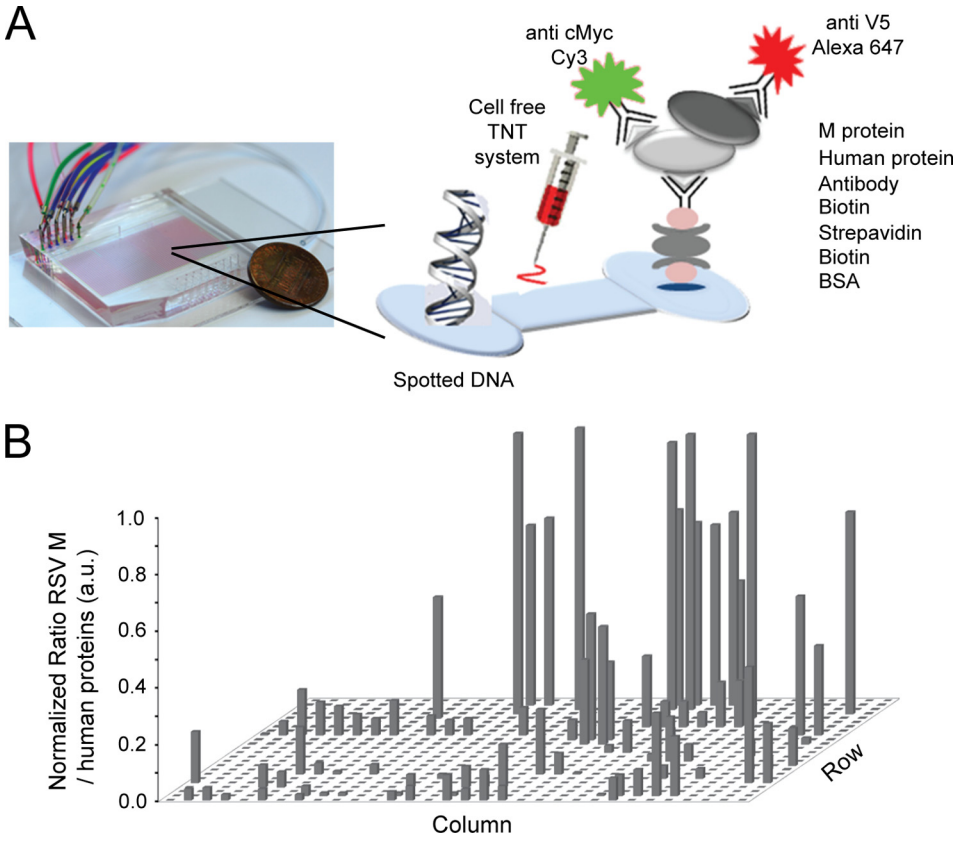

FIG. 1. **A novel microfluidics screen for interactors of RSV M protein.** *A*, Schematic showing details of the screen. DNAs encoding human ORFs with N-terminal c-Myc and C-terminal Penta-His tags were expressed *in vitro* using TNT (transcription and translation mix). Biotinylated BSA was bound to the surface within the microfluidic device to enable strepavidin to form a sandwich between the surface-bound BSA and biotinylated anti-Penta-His antibody, to enable expressed human proteins to be immobilized onto the surface via the Penta-His tag. RSV M was produced separately with a V5 tag at the C terminus, and then flowed into the device and incubated in the reaction chamber to allow binding to human proteins. Interaction was detected by labeling human proteins with Cy3-labeled anti-c-Myc antibody and by labeling M with fluorescent Alexa Fluor 647 anti-V5. *B*, Results of microfluidics screen for RSV M interaction with human proteins. Proteins were immobilized and fluorescently labeled as per *A*. Results are shown for a representative assay (matrix of 32 columns and 24 rows) for 500 human proteins. Each bar represents an average of eight replicates, with an additional 268 spots lacking DNAs serving as negative controls. The X and Y axes represent the coordinates in the two dimensional protein arrays. Only signals with three standard deviations above the negative background level were scored as positive for protein expression. Interaction was defined as the ratio between the fluorescence signals for M (detected with Alexa Fluor 647) and the human protein (detected with Cy3), and normalized relative to the highest ratio. Signals with two standard deviations above negative background were scored as hits.

tails) using RSV M as a prey to identify interactors from a custom library of 500 specific human genes. Encoded proteins were expressed on chip from cDNAs and immobilized on the chip surface (see schematic in Fig. 1*A*). RSV M protein was expressed separately using a coupled *in vitro* transcription/translation system, and subsequently flowed over the chip using the microfluidics plumbing. Protein immobilization through the C terminus and labeling through the N terminus ensures that only full-length proteins are tested. The custom library included genes from pathways reported to be involved in the replication of RSV and related viruses. All genes were analyzed as replicates of eight in each screen (each bar represents an average signal of eight replicates of each protein), with chambers lacking cDNAs serving as negative (background) controls. Only results for cDNAs showing an average expression level of three standard deviations or more above the average background signal (80% of the cDNAs in the screen, see supplemental Table S1) were scored for interaction. Interaction is defined as the ratio between fluorescence signal of M (detected with Alexa Fluor 647) and fluorescence signal of the expressed human protein (detected with Cy3), with the value subsequently normalized by dividing the values by the highest average value obtained for interaction. Hits were scored where signals were two standard deviations above background.

The screen was performed four times, with the results of a typical screen shown in Fig. 1*B*, where the data points represent the average signal for the eight replicates for each protein. Ninety-three of the expressed proteins gave a ratio of two standard deviations above background once or more (see supplemental Table S1). The majority of these were proteins involved in cellular transcription and mRNA translation and

TABLE I
Interactors of RSV M identified in the microfluidics screen

Gene	UniProtKB	Protein name	Positive screens	Function
ACP1	P24666	Acid Phosphatase 1	2	Protein tyrosine phosphatase
AMOT	Q4VCS5	Angiomotin	4	Tight junction maintenance; endothelial cell migration
AmotL2	Q9Y2J4	Angiomotin like protein 2	3	Actin filament regulation; Wnt/β-catenin signaling
Cav2	P51636	Caveolin 2	2	Caveolae formation; MAPK signaling; MAPK1 and STAT3 activation
Cav3	P56539	Caveolin 3	2	Caveolae formation
CFL1	P23528	Cofilin 1	3	Actin dynamics; F-actin depolymerization; cell morphology; regulation of transcription
HIST1H4	P62805	Histone core protein 4	2	Core component of nucleosome
HSPB2	Q16082	Small heat shock protein 27	2	Regulation of DMPK kinase
KPNA2	P52292	Importin α1 (Rch1)	2	NLS-recognising adaptor protein mediating nuclear import
PIK3CB	P42338	Phosphatidylinositol 4,5 bisphosphate 3 kinase catalytic subunit β	3	Cell growth; immune response; cell motility and morphology
PIK3CG	P48736	Phosphatidylinositol 4,5 bisphosphate 3 kinase catalytic subunit γ	3	Cell growth, immune response, cell motility and morphology
PPIA	P62937	Cyclophilin A	2	Accelerates protein folding
PTMA	P06454	Prothymosin α	2	Mediates immune function
Rab11a	P62491	Ras related protein Rab11a	3	Intracellular membrane trafficking, epithelial cell polarization
Rab11b	Q15907	Ras related protein Rab11b	2	Intracellular membrane trafficking
EXOC6	Q8TAG9	Exocyst Complex Component 6	2	Vesicular trafficking from the Golgi to plasma membrane
SMAD3	P84022	SMAD family member 3	2	Transcriptional regulator activated by TGF-β
SUMO3	P55854	Small Ubiquitin-like modifier 3	3	Adaptor molecule involved in nuclear transport, DNA replication, signal transduction
Tom22	Q9NS69	Translocase of outer mitochondrial membrane 22 homolog	2	Mediates transport into the mitochondria of cytoplasmically synthesized proteins
TUBA6	Q9BQE3	Tubulin α	2	Major component of microtubules
VDAC1	P21796	Voltage dependent anion channel 1	2	Mitochondrial outer mitochondrial membrane channel protein; implicated in apoptosis
ZCCHC7	Q8N3Z6	CCHC domain-containing zinc finger protein 7	2	Component of the nucleolar TRAMP-like complex
ZNF501	Q96CX3	Zinc finger protein 501	2	DNA/zinc ion binding; involved in transcriptional regulation ?
ZNF502	Q8TBZ5	Zinc finger protein 502	2	DNA/zinc ion binding; involved in transcriptional regulation ?

Abbreviations: Wingless-type (Wnt), mitogen-activated protein kinase (MAPK), signal transducer and activator of transcription 3 (STAT3), dystrophy myotonic protein kinase (DMPK), nuclear localization signal (NLS), rat sarcoma (RAS), transforming growth factor (TGF), translocation associated membrane protein (TRAMP).

splicing regulation, signaling and trafficking pathways, and cytoskeleton related proteins. Table I lists 24 novel binding partners for M that scored positive in two or more screens.

RSV M Host Interactions Verified—A selection of the hits was evaluated in more detail using a smaller microfluidic device (Fig. 2*A*) (see Experimental Procedures for details), whereby human proteins were expressed in the presence of fluorescent Lys (FluoroTect™ GreenLys) with C-terminal Penta-His to ensure that the N-terminal Myc tag is not impacting on proper folding of the protein. Based on the close homology and similar functional role of Cav1 to Cav2/3, Cav1 (not in the original screen) was also tested in these experiments, together with the proteasomal regulator Psme3 (PA28) and green fluorescent protein (GFP) as negative controls. All of the hits (as well as Cav1), showed substantial and specific binding to M under the tested conditions (Fig. 2*A*).

We then validated a number of the interactions in coimmunoprecipitation experiments in 293T cells using expression constructs for Myc-tagged cellular factor and OSF-tagged RSV M (Fig. 2*B*); in this assay RSV M was captured onto affinity beads while the cellular protein was in the lysate, in contrast to the binding setup in the microfluidics systems. M2–1, previously shown to interact with M in a cell-free system (10), was used as positive control; additionally, because RSV M is known to form higher order oligomers, we also used this as a positive control (17, 18). As is evident from Fig. 2*B*, Myc-M2–1 coprecipitated specifically with OSF-M, as did (from left to right in the top panel) Myc-M, -Cav1, -Cav3, -Cof1, -ZNF502, and -Tom22, whereas Myc-Rab11b, and-AmotL2 did not. Importantly, Cav1, Cav3, Cof1, ZNF502, and Tom22 were all able to interact with RSV M in intact cells. Overall, five out of seven interactions (71%) were confirmed using the coimmunoprecipitation assay.

For further experiments, we decided to focus on the actin-binding protein Cof1, and Cav1, which as a heterodimer with Cav2, is a key component of the caveolae membrane struc-

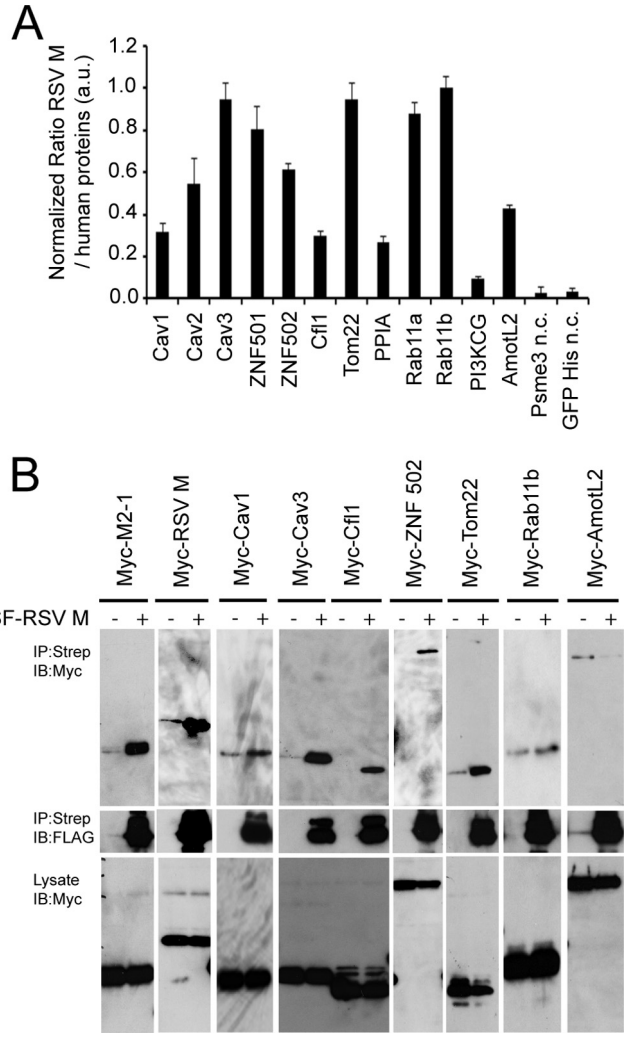

FIG. 2. **Validation of hits for interaction with RSV M.** *A*, Hit validation using a small scale microfluidics affinity assay. The assay was performed as described in the Methods section, with GFP and PSME3 (PA28) as negative controls (n.c.). As in Fig. 1*B*, Interaction is defined as the ratio between the fluorescence signals for M and the indicated protein, and normalized relative to the highest ratio. All ratios were significantly different ($p < 0.001$, Mann-Whitney nonparametric test) from the negative controls. *B*, RSV M associates with host factors in transfected 293T cells. Cells were transfected to express the indicated Myc-tagged proteins together with empty vector (−) or OSF-tagged RSV M protein (+). Cells were lysed 36 h post transfection and subjected to pull-down using Streptactin Sepharose. Proteins were detected by Western analysis using anti-Myc or anti-FLAG primary antibodies followed by goat anti-mouse HRP-conjugated secondary antibodies. Upper panel: Myc-tagged proteins coprecipitations with empty vector controls (−) and OSF-RSV M (+). Middle and lower panels: OSF-RSV M binding to Streptactin Sepharose and Myc-tagged proteins expression in cell lysates, respectively.

tures that are believed to be important for RSV filament formation. Cav3, which has amino acid sequence similar to Cav1, was not included because it is mostly expressed in muscle cells (32), which are not relevant for RSV infection. In addition, because our hits included a number of transcription factors, including several zinc finger proteins that may be targets of RSV M transcriptional inhibition (6) (Table II), we selected zinc finger protein ZNF502 for further analysis. ZNF502 was also identified as a binding partner of M using mass spectrophotometric approach (data not shown).

RSV Colocalizes with Cav1 and Cofilin1 Proteins in Virus-like Structures—In order to validate whether the identified proteins colocalize with M within RSV-like structures, we used our previously described VLP transfection based assay (Fig. 3). To analyze the subcellular localization of the host proteins in the absence of RSV proteins, HEp-2 cells were transfected to express Myc-tagged CHMP1B, -M2–1, -Cav1, -Cof1, or -ZNF502, where CHMP1B served as a negative control based on the screening results, and M2–1 was the positive control (see above). Cells were fixed and stained with anti-Myc antibodies 24 h post-transfection (Fig. 3*A*), with Myc-CHMP1B found to localize to endosomal membranes as previously observed (33) and Myc-M2–1 showing a cytoplasmic distribution. Myc-Cav1 localized into caveolae structures at the plasma membrane, Myc-Cof1 was cytoplasmic, possibly associated with the cytoskeleton, and Myc-ZNF502 was nuclear. To analyze colocalization in the presence of RSV proteins, HEp-2 cells were cotransfected with codon-optimized vectors expressing RSV F, N, P, and M protein, together with the plasmids encoding the Myc-tagged proteins as in Fig. 3*A*. Cells were fixed and stained with anti-RSV in addition to anti-Myc antibodies 24 h post transfection (Fig. 3*B*). As expected, Myc-CHMP1B showed no alteration in localization in the presence of RSV proteins, whereas Myc-M2–1 showed striking colocalization with RSV proteins in inclusions, in stark contrast to its localization in the absence of RSV proteins. In the presence of RSV proteins, Myc-Cav1 was observed to localize at the base of virus-like filaments, whereas Myc-Cof1 relocalized to large inclusions (see (34)).

M Relocates to the Nucleus in the Presence of Ectopically Expressed ZNF502—In contrast to the above, Myc-ZNF502 appeared to remain predominantly nuclear even in the presence of RSV proteins (Fig. 3*B*). To assess whether ZNF502 might affect M subcellular localization, we performed the same experiment but instead staining for M specifically (Fig. 3*C*). In the absence of Myc-ZNF502, M was predominantly associated with the virus-like filaments, but in its presence, M localization appeared to change. M demonstrated reduced association with filaments, and instead increased localization in both cytoplasm and nucleus.

Cav1 and Cof1 Localize in Viral Structures in RSV Infected Cells—To extend the results to infected cells, we performed immunofluorescence on BEAS-2B cells infected with WT A2 virus and stained for RSV and endogenous Cav1, Cav2, or Cof1 (Fig. 4*A*). Results were comparable to those above; in mock infected cells (upper panel), endogenous Cav1 and Cav2 localized into caveolae structures whereas Cof1 was cytoplasmic. In infected cells, RSV proteins colocalized with Cav1 and Cav2 in viral filaments, whereas Cof1 relocalized

TABLE II
Zinc finger proteins identified as interactors of RSV M

Gene	Protein name	Number and type of zinc fingers	Function
Trim27	Tripartite Motif Containg 27	3, RING and B box	Transcription repression, E3 ligase of PIK3C2B, inhibition of CD4 activation
YY1	Yin and Yang 1	4, GLI Kruppel	Transcription repression
ZCCHC7	Zinc finger CCHC domain containing 7	4, CCHC	RNA exosome
ZNF501	Zinc finger protein 501	9, C2H2	Presumably transcription regulation
ZNF502	Zinc finger protein 502	14, C2H2	Presumably transcription regulation
ZMYM6	Zinc finger MYM type 6	8, MYM	Cell morphology and cytoskeleton
ZNF410	Zinc finger protein 410	5, C2H2	Transcription factor
NR2C2	Nuclear receptor subfamily 2, group C	2, NR-C4	Transcription repression

Abbreviation: Phosphatidylinositol 4,5 bisphosphate 3 kinase catalytic subunit β (PIK3C2B).

into viral IBs (lower panel). Western analysis indicated that Cav1 and Cav2 levels did not change up to 48 h postinfection compared with mock-infected cells, whereas Cof1 levels were reduced in the soluble fraction in infected cells (Fig. 4*B*), most probably because of relocalization into IBs, which are not soluble in the buffer used.

In summary, Cav1, Cav2, and Cof1 subcellular localization was altered in the presence of RSV proteins, and showed marked colocalization with viral components, consistent with a direct interaction with RSV M, whereas ectopically expressed ZNF502 appears to change subcellular localization of M specifically, implying a role in facilitating M nuclear localization and/or retention.

Cof1, ZNF502, and Cav2 are Required for Optimal RSV Virus Production—siRNA depletion experiments were performed to test whether host proteins identified as interacting with M play a role in RSV replication (Fig. 5). HEp-2 cells were transfected with control scrambled siRNA or siRNA specifically targeting Cof1 or Cav1 and/or Cav2, with siRNA to the host gene CK2α included as a positive control (17). 293T cells were used for the ZNF502 knockdown experiments due to the fact that HEp-2 cells exhibited low expression levels of ZNF502 protein (data not shown). 48 h post-transfection, cells were infected with WT RSV at an MOI of three, and cell associated virus was harvested for plaque assay 24 h later. Protein levels after knockdown are shown in Fig. 5*A* and 5*C*, with β actin as a loading control. As shown in Fig. 5*B*, depletion of CK2α resulted in an up to 60% reduction in cell-associated virus as previously reported (17). Depletion of Cof1 yielded a comparable (50%) reduction in infectious virus production. ZNF502 depletion resulted in 60% reduction in cell-associated virus (Fig. 5*B*, *upper* panel) and about the same level of reduction of released virus (Fig. 5*B*, *lower* panel). Thus, ZNF502, like Cof1, is required for optimal RSV virus production. The fact that siRNA depletion of Cof1 and ZNF502 did not completely ablate virus production is attributable to the fact that knockdown of the respective genes (65% for both Cof1 and ZNF502) was not complete.

The human Caveolin proteins, of which Cav1 and 2 are ubiquitous but Cav3 is largely muscle-specific are essential structural components of caveolae (32). Cav2 and Cav3 were both identified as hits in our screens (Table I) with Cav1–3 all showing interaction with RSV M (Fig. 2). Importantly, we observed colocalization of endogenous Cav1 and Cav2 with viral filaments (Fig. 3*B* and Fig. 4*A*) raising the question as to whether Cav proteins may be required either for viral filament formation or viral infectivity. To test this, HEp-2 cells were transfected with siRNA specifically targeting Cav1, Cav2, or both with scrambled siRNA serving as control, and cells were infected with WT RSV at an MOI of three 48 h later. Knockdown of Cav1 alone (90% reduction) had no significant impact on cell-associated virus titer. In contrast, depletion of Cav2 (80% reduction) or Cav1 and Cav2 simultaneously (65 and 90%, respectively) resulted in up to 70% reduction in virus titer (Fig. 5*D*, *upper* panel). We also checked whether depletion of Cav proteins affect released virus infectivity. Knockdown of Cav2 alone resulted in significant reduction in viral titer (Fig. 5*D*, *lower* panel).

Because depletion of Cav2 seemed to affect virus titer both in cell-associated and released virus fraction, we tested whether RSV filaments still formed in Cav-depleted cells. HEp-2 cells were transfected with siRNA specifically targeting Cav1, Cav2, or control scrambled siRNA, and infected with WT RSV at an MOI of three 48 h later. Cells were subsequently fixed 24 h later, and stained with antibodies specific for Cav1 or Cav2 and RSV M protein. Endogenous Cav1 and Cav2 were found to colocalize with the viral filaments in RSV-infected cells, in agreement with staining in BEAS-2B cells (Fig. 4*A*). Significantly, however, viral filaments still formed in Cav1-depleted and in Cav2-depleted and RSV-infected cells (supplemental Fig. S1).

DISCUSSION

This study is the first to use microfluidics technology to perform a high-throughput screen to identify 24 novel host factors that can interact directly with the RSV M protein (see Table I). Further, although previous proteomics-based studies have identified host cell factors important for RSV replication, this is the first to identify and validate host proteins directly interacting with RSV M. Here, we focused on three selected

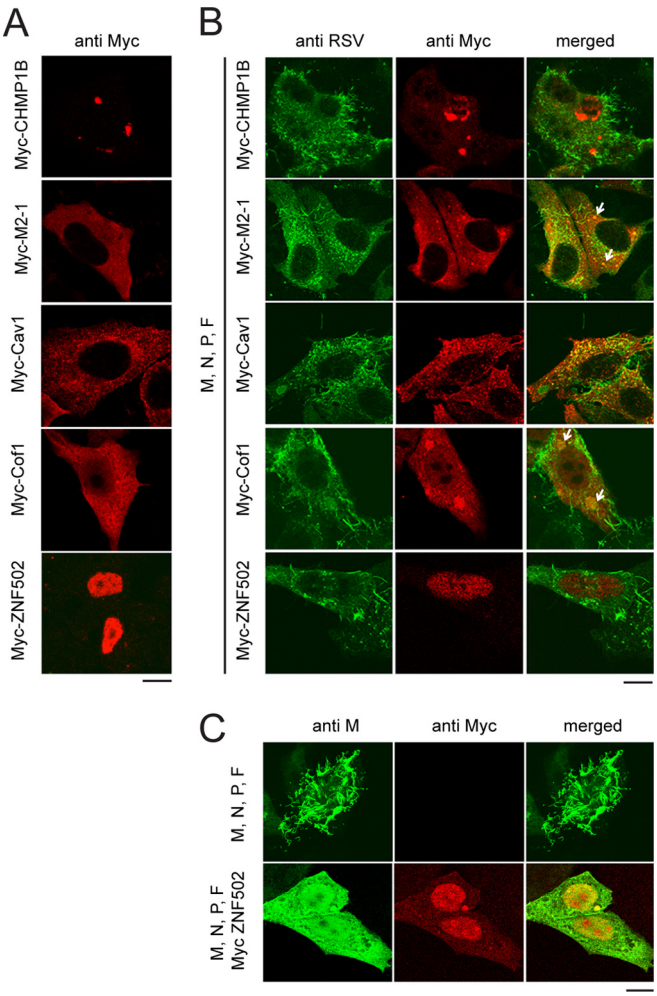

FIG. 3. ***A*, Subcellular localization of interactors of M in the absence and presence of RSV proteins.** HEp-2 cells were transfected to express the indicated Myc-tagged proteins, fixed, and permeabilized 24 h post transfection, and then immunostained using anti-Myc monoclonal followed by Alexa Fluor 568-coupled donkey anti-mouse secondary antibodies, and analyzed by confocal microscopy. *B*, Colocalization of host factors with RSV viral structures. HEp-2 cells were cotransfected with pcDNA3.1 plasmids encoding RSV P, N, F, and M proteins together with the indicated pCAG encoded Myc-tagged proteins. Cells were fixed, permeabilized 24 h post transfection and immunostained with anti-RSV polyclonal and anti-Myc monoclonal primary antibodies, followed by Alexa Fluor 488-coupled rabbit anti-goat and Alexa Fluor 568-coupled donkey anti-mouse secondary antibodies and analyzed by confocal microscopy. *C*, Relocalization of M in the presence of ectopically expressed ZNF502. HEp-2 cells were cotransfected with pcDNA3.1 plasmids encoding RSV P, N, F, and M proteins with or without pCAG Myc-ZNF502. Cells were fixed, permeabilized 24 h post transfection and immunostained with anti-M monoclonal and anti-Myc polyclonal followed by Alexa Fluor 488-coupled goat anti-mouse and Alexa Fluor 568-coupled goat anti-rabbit secondary antibodies and analyzed by confocal microscopy. Scale bars represent 10 μm.

hits in particular, characterizing their colocalization with RSV proteins and their effect on RSV replication.

We showed that M can interact with all three members of the Caveolin family (Fig. 2 and Table I). Together with cellular colocalization of Cav1 and Cav2 with M at the viral filaments (Figs. 3*B* and 4*A*), this implies that interaction with Caveolin proteins occurs in lipid rafts at the plasma membrane where M oligomerizes and virion budding takes place, and presumably it is the mechanism by which Cav1 can be incorporated into mature virions. Lipid raft integrity has been shown to be essential for proper RSV assembly and release of infectious particles (35–38), with Cav1, an integral component of lipid rafts, shown to be incorporated into mature virions (34, 37). Importantly, our results showed that depletion of Cav2 rather than Cav1 by siRNA has a significant effect on infectivity of both cell-associated and released virus (Fig. 5*D*). Based on our results showing that RSV filaments were still formed in Cav1 and Cav2 depleted RSV infected cells (supplemental Fig. S1), we speculate that lipid rafts and Caveolin proteins may be required for optimal infectivity of the released RSV viral particles, similar to what has been demonstrated for Newcastle disease virus (NDV) (39). One possibility is that lipid raft integrity, dependent on Cav1/2, is required for viral filament stability. Intriguingly, even though Cav1/2 form heterodimers and are both key components of lipid rafts, only depletion of Cav2 impacted significantly on RSV infectivity. An exciting possibility is that in RSV assembly Cav2 plays a role distinct to that of Cav1 out of the context of the Cav1/2 heterodimer, but this remains to be tested experimentally.

We also validated the actin-binding protein Cof1 as a host factor interacting with M both *in vitro* (Table I and Fig. 2*A*), and in transfected cells (Fig. 2*B*). We showed that Cof1 localizes into RSV IBs in transfected and in RSV-infected cells (Fig. 3*B* and Fig. 4*A*) (see (34)). Cof1 has also been shown previously to be incorporated into mature virions (34), and our work suggests that the incorporation of Cof1 into the virions may be through direct association of M and Cof1. The fact that knocking down Cof1 results in a 50% reduction of infectious virus indicates that Cof1-M interaction plays an essential role in RSV replication. Actin integrity has been shown to be important during RSV infection, presumably through involvement in filament formation (40), where cytoskeletal proteins have been suggested to be involved in the transport of the viral RNP to the sites of budding, which is dependent on M (16). Interestingly, independently of its role as cytoskeleton protein, actin has been shown to be able to act as a transcriptional modulator through binding to the RSV template (41). Our colocalization experiments show that in RSV-infected cells, Cof1 relocalizes into viral IBs resulting in reduction in Cof1 levels in the cytoplasm (Fig. 4*B*). We speculate that M may sequester Cof1 in IBs in order to impact on actin polymerization, resulting in an increase of F actin filaments, which could either facilitate trafficking of RSV proteins or viral transcription in IBs. Further work will be required to establish the precise role of RSV M-Cof1 interaction in RSV infection.

Significantly, our microfluidics screen identified a total of eight ZNF-containing proteins, mostly transcription factors, as interactors of RSV M (Table II). We focused on ZNF502,

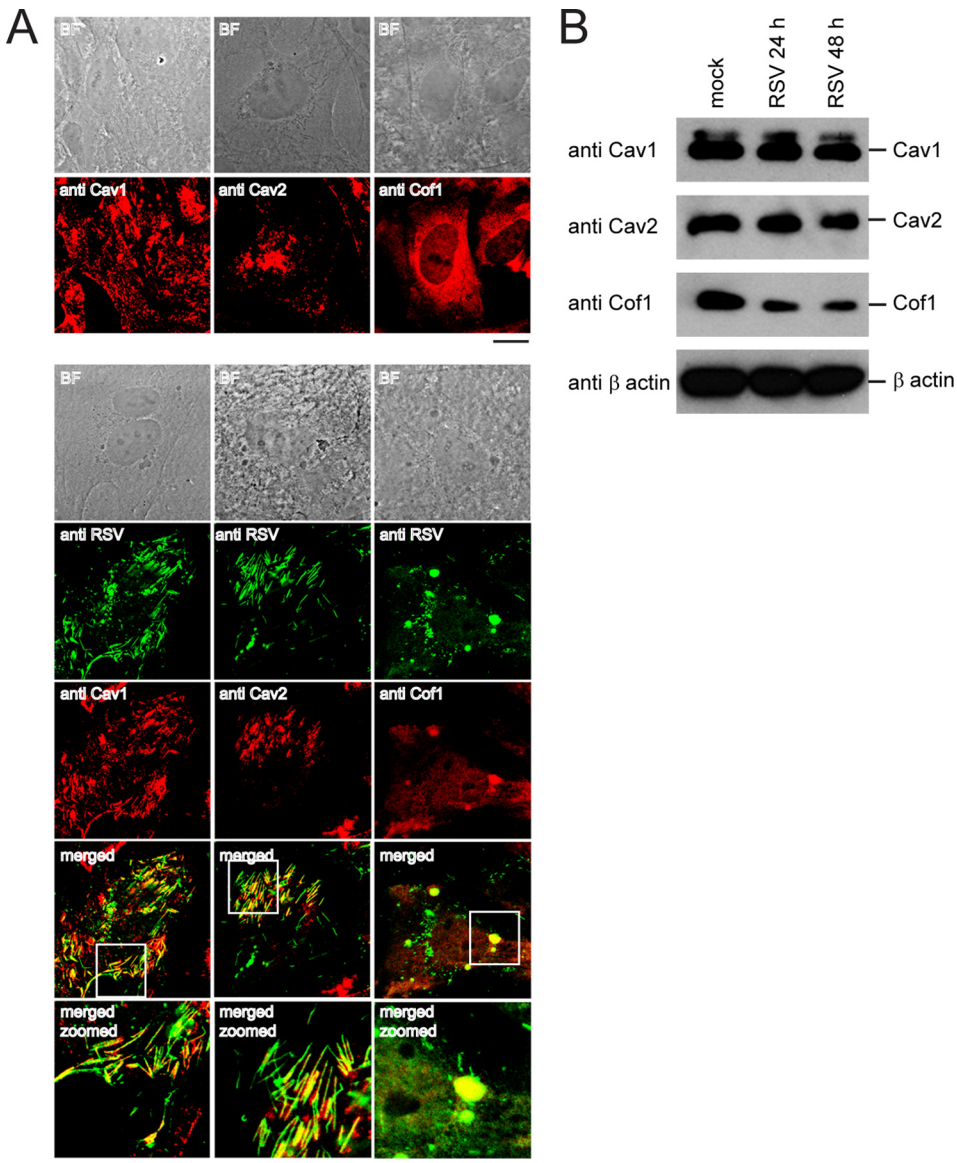

FIG. 4. **RSV colocalizes with Cav1, Cav2, and Cofilin1 proteins in viral structures in infected cells.** *A*, BEAS-2B cells were seeded at 4×10^5 cells/well in 6-well plate with glass cover slips followed by WT A2 RSV infection (MOI of three) 24 h later. Cells were fixed 24 h postinfection, permeabilized and immunostained with anti-RSV polyclonal and anti-Cav1, anti-Cav2 or anti-Cof1 polyclonal antibodies and Alexa Fluor 488-coupled goat anti-mouse and Alexa Fluor 568-coupled goat anti-rabbit secondary antibodies and analyzed by confocal microscopy. Scale bar represent 10 μm. *B*, Host proteins levels in RSV-infected cells. Cell lysates were prepared 24 h postinfection in RIPA buffer and subjected to Western analysis using the indicated primary antibodies together with anti-rabbit HRP-conjugated secondary antibody.

showing direct interaction with M both *in vitro* and in transfected cells (Fig. 2). Importantly, partial knockdown of ZNF502 in 293T cells resulted in a 60% reduction of cell associated and 70% reduction of released infectious virus (Fig. 5*B*). Strikingly, ectopic expression of ZNF502 appeared to increase M nuclear accumulation and decrease viral filament formation (Fig. 3*C*). Further work is required to determine the precise contribution of ZNFs such as ZNF502 in RSV infection, and the extent to which this may impact on M transcriptional inhibition, or other activities of M.

Additional to the three host factors above, direct interactors with M included Rab11a, Rab11b, and Sec15, all of which are involved in vesicular trafficking, with Rab11a previously having been shown to be critical for RSV filament formation and infectivity (24). Although Rab11a and Rab11b interacted with M in the microfluidics system, the M-Rab11b interaction could not be verified by coimmunoprecipitation (Fig. 2*B*). Although this implies that the interactions may not occur in the intact cell, the lack of validation may be attributable to the fact that our microfluidics platform measures interactions at equilibrium. Consequently, the platform is sensitive to weak interactions and to strong interactions with fast off rates. Apart from Rab11a/11b, our hits also included two catalytic subunits (PI3KCB and PI3KCG) of phosphatidylinositol-4,5-bisphos-

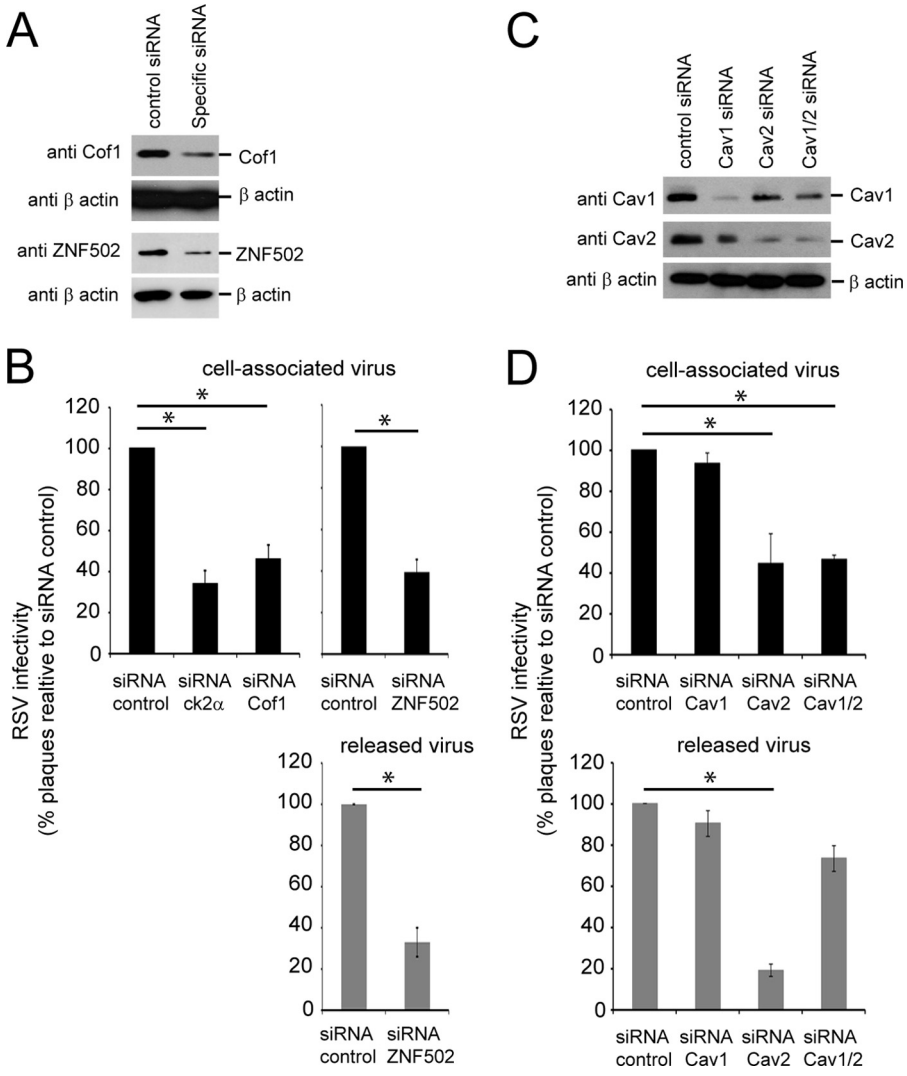

FIG. 5. **Depletion of Cof1, Cav2, and ZNF502 negatively affects RSV replication.** 4 × 10^5 HEp-2 cells were seeded per well in 6-well plates and transfected with control scrambled or specific siRNA (20 nM) 24 h later, followed by WT A2 RSV infection (MOI of three) 48 h post transfection. 293T cells were used for ZN502. *A* and *C*, Cell lysates were prepared in RIPA buffer 24 h postinfection and subjected to Western analysis using the indicated primary antibodies together with anti-rabbit HRP-conjugated secondary antibody. *B* and *D*, Cell-associated or released virus was harvested 24 h postinfection. Virus titer was either determined on HEp-2 cells using an immune-plaque, or by plaque assay on Vero cells as described in the Methods section. Results represent the mean ± S.D. ($n = 3$), expressed as a % compared with negative control. (see Experimental procedures). * $p < 0.05$.

phate 3-kinase (PI3K), previously shown to be involved in the innate immune response in RSV infection (42, 43). PI3K levels are known to increase in RSV infected cells, which may impact on RSV filament formation (44); whether interaction with M may serve to localize PI3K kinase activity at the site of viral assembly is unclear, but we are currently using specific PI3K inhibitors to test their effect on RSV replication. Further hits included Tom22 (validated in co-IP) and VDAC1, mitochondrial proteins involved in the innate immune response, whose levels and cellular localization change during RSV infection (45). Further work will be required to delineate the exact molecular mechanism of each of these interactions and their effect on RSV replication.

In summary, our novel screening approach has identified a number of new potential host targets for RSV M, shedding light on the cellular mechanisms utilized by RSV for its replication. The host interactors are from a variety of cellular pathways involved in transcription, translation, trafficking, innate immunity signaling and assembly, reflecting the multi functionality and the ability of viral proteins, and RSV M in particular, to target multiple host proteins. Future work is focused on detailed analysis of the mechanism for the binding interactions, with important potential as targets for antiviral therapy.

* This work was supported by institutional funds (ID#707999) from Imperial College, by a Marie Curie Career Integration Grant (#321931) from European Commission (MB), by project grants (ID#606407 and APP1043511) and a fellowship (APP1002486) from the National Health and Medical Research Council, Australia (DAJ), by research grants (#3309600) from European Research Council and (#715-11) from Israel Science Foundation (DG).

S This article contains supplemental Fig. S1 and Table S1.

** To whom correspondence should be addressed: Nanotechnology Institute, Mina and Evrard Goodman Faculty of Life Sciences, Anna Web Nanotechnology bld. (206), Bar Ilan University, Ramat Gan, Israel 5290002. Tel.: +97237384509; Fax: +97237384196; E-mail: Doron.Gerber@biu.ac.il. Section of Virology, Faculty of Medicine, Imperial College London, London, UK. Tel.: +44 (0)20 759 41124; Fax: +44 (0)20 759 43973; E-mail: m.bajorek@imperial.ac.uk.

‡‡ Corresponding authors.

REFERENCES

1. Collins, P. L., and Graham, B. S. (2008) Viral and host factors in human respiratory syncytial virus pathogenesis. *J. Virol.* **82,** 2040–2055
2. Falsey, A. R., Hennessey, P. A., Formica, M. A., Cox, C., and Walsh, E. E. (2005) Respiratory syncytial virus infection in elderly and high-risk adults. *New Engl. J. Med.* **352,** 1749–1759
3. Sidwell, R. W., and Barnard, D. L. (2006) Respiratory syncytial virus infections: recent prospects for control. *Antiviral Res.* **71,** 379–390
4. Guvenel, A. K., Chiu, C., and Openshaw, P. J. (2014) Current concepts and progress in RSV vaccine development. *Expert Rev. Vaccines* **13,** 333–344
5. Ghildyal, R., Ho, A., Wagstaff, K. M., Dias, M. M., Barton, C. L., Jans, P., Bardin, P., and Jans, D. A. (2005) Nuclear import of the respiratory syncytial virus matrix protein is mediated by importin beta1 independent of importin alpha. *Biochemistry* **44,** 12887–12895
6. Ghildyal, R., Baulch-Brown, C., Mills, J., and Meanger, J. (2003) The matrix protein of Human respiratory syncytial virus localises to the nucleus of infected cells and inhibits transcription. *Arch. Virol.* **148,** 1419–1429
7. Ghildyal, R., Mills, J., Murray, M., Vardaxis, N., and Meanger, J. (2002) Respiratory syncytial virus matrix protein associates with nucleocapsids in infected cells. *J. Gen. Virol.* **83,** 753–757
8. Ghildyal, R., Ho, A., Dias, M., Soegiyono, L., Bardin, P. G., Tran, K. C., Teng, M. N., and Jans, D. A. (2009) The respiratory syncytial virus matrix protein possesses a Crm1-mediated nuclear export mechanism. *J. Virol.* **83,** 5353–5362
9. Lifland, A. W., Jung, J., Alonas, E., Zurla, C., Crowe, J. E., Jr., and Santangelo, P. J. (2012) Human respiratory syncytial virus nucleoprotein and inclusion bodies antagonize the innate immune response mediated by MDA5 and MAVS. *J. Virol.* **86,** 8245–8258
10. Li, D., Jans, D. A., Bardin, P. G., Meanger, J., Mills, J., and Ghildyal, R. (2008) Association of respiratory syncytial virus M protein with viral nucleocapsids is mediated by the M2–1 protein. *J. Virol.* **82,** 8863–8870
11. Baviskar, P. S., Hotard, A. L., Moore, M. L., and Oomens, A. G. (2013) The respiratory syncytial virus fusion protein targets to the perimeter of inclusion bodies and facilitates filament formation by a cytoplasmic tail -dependent mechanism. *J. Virol.* **87,** 10730–10741
12. Roberts, S. R., Compans, R. W., and Wertz, G. W. (1995) Respiratory syncytial virus matures at the apical surfaces of polarized epithelial cells. *J. Virol.* **69,** 2667–2673
13. Harrison, M. S., Sakaguchi, T., and Schmitt, A. P. (2010) Paramyxovirus assembly and budding: building particles that transmit infections. *Int. J. Biochem. Cell Biol.* **42,** 1416–1429
14. Shaikh, F. Y., Cox, R. G., Lifland, A. W., Hotard, A. L., Williams, J. V., Moore, M. L., Santangelo, P. J., and Crowe, J. E., Jr. (2012) A critical phenylalanine residue in the respiratory syncytial virus fusion protein cytoplasmic tail mediates assembly of internal viral proteins into viral filaments and particles. *mBio* **3(1),** pii:e00270–11
15. Oomens, A. G., Bevis, K. P., and Wertz, G. W. (2006) The cytoplasmic tail of the human respiratory syncytial virus F protein plays critical roles in cellular localization of the F protein and infectious progeny production. *J. Virol.* **80,** 10465–10477
16. Mitra, R., Baviskar, P., Duncan-Decocq, R. R., Patel, D., and Oomens, A. G. (2012) The human respiratory syncytial virus matrix protein is required for maturation of viral filaments. *J. Virol.* **86,** 4432–4443
17. Bajorek, M., Caly, L., Tran, K. C., Maertens, G. N., Tripp, R. A., Bacharach, E., Teng, M. N., Ghildyal, R., and Jans, D. A. (2014) The Thr205 Phosphorylation site within respiratory syncytial virus matrix (M) protein modulates m oligomerization and virus production. *J. Virol.* **88,** 6380–6393
18. Liljeroos, L., Krzyzaniak, M. A., Helenius, A., and Butcher, S. J. (2013) Architecture of respiratory syncytial virus revealed by electron cryotomography. *Proc. Natl. Acad. Sci. U.S.A.* **110,** 11133–1138
19. Kiss, G., Holl, J. M., Williams, G. M., Alonas, E., Vanover, D., Lifland, A. W., Gudheti, M., Guerrero-Ferreira, R. C., Nair, V., Yi, H., Graham, B. S., Santangelo, P. J., and Wright, E. R. (2014) Structural analysis of respiratory syncytial virus reveals the position of M2–1 between the matrix protein and the ribonucleoprotein complex. *J. Virol.* **88,** 7602–7617
20. Craven, R. C., Harty, R. N., Paragas, J., Palese, P., and Wills, J. W. (1999) Late domain function identified in the vesicular stomatitis virus M protein by use of rhabdovirus-retrovirus chimeras. *J. Virol.* **73,** 3359–3365
21. Harty, R. N., Paragas, J., Sudol, M., and Palese, P. (1999) A proline-rich motif within the matrix protein of vesicular stomatitis virus and rabies virus interacts with WW domains of cellular proteins: implications for viral budding. *J. Virol.* **73,** 2921–2929
22. Schmitt, A. P., Leser, G. P., Morita, E., Sundquist, W. I., and Lamb, R. A. (2005) Evidence for a new viral late-domain core sequence, FPIV, necessary for budding of a paramyxovirus. *J. Virol.* **79,** 2988–2997
23. Ciancanelli, M. J., and Basler, C. F. (2006) Mutation of YMYL in the Nipah virus matrix protein abrogates budding and alters subcellular localization. *J. Virol.* **80,** 12070–12078
24. Brock, S. C., Goldenring, J. R., and Crowe, J. E., Jr. (2003) Apical recycling systems regulate directional budding of respiratory syncytial virus from polarized epithelial cells. *Proc. Natl. Acad. Sci. U.S.A.* **100,** 15143–15148
25. Utley, T. J., Ducharme, N. A., Varthakavi, V., Shepherd, B. E., Santangelo, P. J., Lindquist, M. E., Goldenring, J. R., and Crowe, J. E., Jr. (2008) Respiratory syncytial virus uses a Vps4-independent budding mechanism controlled by Rab11-FIP2. *Proc. Natl. Acad. Sci. U.S.A.* **105,** 10209–10214
26. Oliveira, A. P., Simabuco, F. M., Tamura, R. E., Guerrero, M. C., Ribeiro, P. G., Libermann, T. A., Zerbini, L. F., and Ventura, A. M. (2013) Human respiratory syncytial virus N, P, and M protein interactions in HEK-293T cells. *Virus Res.* **177,** 108–112
27. Chen, R., and Snyder, M. (2010) Yeast proteomics and protein microarrays. *J. Proteomics* **73,** 2147–2157
28. Gerber, D., Maerkl, S. J., and Quake, S. R. (2009) An in vitro microfluidic approach to generating protein-interaction networks. *Nat. Methods* **6,** 71–74
29. Fordyce, P. M., Gerber, D., Tran, D., Zheng, J., Li, H., DeRisi, J. L., and Quake, S. R. (2010) De novo identification and biophysical characterization of transcription-factor binding sites with microfluidic affinity analysis. *Nat. Biotechnol.* **28,** 970–975
30. Glick, Y., Avrahami, D., Michaely, E., and Gerber, D. (2012) High-throughput protein expression generator using a microfluidic platform. *J. Vis. Exp.* e3849
31. Yang, X., Boehm, J. S., Salehi-Ashtiani, K., Hao, T., Shen, Y., Lubonja, R., Thomas, S. R., Alkan, O., Bhimdi, T., Green, T. M., Johannessen, C. M., Silver, S. J., Nguyen, C., Murray, R. R., Hieronymus, H., Balcha, D., Fan, C., Lin, C., Ghamsari, L., Vidal, M., Hahn, W. C., Hill, D. E., and Root, D. E. (2011) A public genome-scale lentiviral expression library of human ORFs. *Nat. Methods* **8,** 659–661
32. Williams, T. M., and Lisanti, M. P. (2004) The caveolin proteins. *Genome Biol.* **5,** 214
33. Babst, M., Katzmann, D. J., Estepa-Sabal, E. J., Meerloo, T., and Emr, S. D. (2002) Escrt-III: an endosome-associated heterooligomeric protein complex required for mvb sorting. *Dev. Cell* **3,** 271–282
34. Radhakrishnan, A., Yeo, D., Brown, G., Myaing, M. Z., Iyer, L. R., Fleck, R., Tan, B. H., Aitken, J., Sanmun, D., Tang, K., Yarwood, A., Brink, J., and Sugrue, R. J. (2010) Protein analysis of purified respiratory syncytial virus particles reveals an important role for heat shock protein 90 in virus particle assembly. *Mol. Cell. Proteomics* **9,** 1829–1848
35. Marty, A., Meanger, J., Mills, J., Shields, B., and Ghildyal, R. (2004) Association of matrix protein of respiratory syncytial virus with the host cell membrane of infected cells. *Arch. Virol.* **149,** 199–210
36. Henderson, G., Murray, J., and Yeo, R. P. (2002) Sorting of the respiratory syncytial virus matrix protein into detergent-resistant structures is dependent on cell-surface expression of the glycoproteins. *Virology* **300,** 244–254
37. McCurdy, L. H., and Graham, B. S. (2003) Role of plasma membrane lipid microdomains in respiratory syncytial virus filament formation. *J. Virol.* **77,** 1747–1756
38. Chang, T. H., Segovia, J., Sabbah, A., Mgbemena, V., and Bose, S. (2012) Cholesterol-rich lipid rafts are required for release of infectious human respiratory syncytial virus particles. *Virology* **422,** 205–213
39. Laliberte, J. P., McGinnes, L. W., Peeples, M. E., and Morrison, T. G. (2006) Integrity of membrane lipid rafts is necessary for the ordered assembly and release of infectious Newcastle disease virus particles. *J. Virol.* **80,** 10652–10662
40. Kallewaard, N. L., Bowen, A. L., and Crowe, J. E., Jr. (2005) Cooperativity of actin and microtubule elements during replication of respiratory syncytial virus. *Virology* **331,** 73–81
41. Harpen, M., Barik, T., Musiyenko, A., and Barik, S. (2009) Mutational analysis reveals a noncontractile but interactive role of actin and profilin

in viral RNA-dependent RNA synthesis. *J. Virol.* **83,** 10869–10876
42. Thomas, K. W., Monick, M. M., Staber, J. M., Yarovinsky, T., Carter, A. B., and Hunninghake, G. W. (2002) Respiratory syncytial virus inhibits apoptosis and induces NF-kappa B activity through a phosphatidylinositol 3-kinase-dependent pathway. *J. Biol. Chem.* **277,** 492–501
43. Bitko, V., Shulyayeva, O., Mazumder, B., Musiyenko, A., Ramaswamy, M., Look, D. C., and Barik, S. (2007) Nonstructural proteins of respiratory syncytial virus suppress premature apoptosis by an NF-kappaB-dependent, interferon-independent mechanism and facilitate virus growth. *J. Virol.* **81,** 1786–1795
44. Yeo, D. S., Chan, R., Brown, G., Ying, L., Sutejo, R., Aitken, J., Tan, B. H., Wenk, M. R., and Sugrue, R. J. (2009) Evidence that selective changes in the lipid composition of raft-membranes occur during respiratory syncytial virus infection. *Virology* **386,** 168–182
45. Munday, D. C., Surtees, R., Emmott, E., Dove, B. K., Digard, P., Barr, J. N., Whitehouse, A., Matthews, D., and Hiscox, J. A. (2012) Using SILAC and quantitative proteomics to investigate the interactions between viral and host proteomes. *Proteomics* **12,** 666–672